Cardiovasc Intervent Radiol (2015) 38:112–120
DOI 10.1007/s00270-014-0900-7

CLINICAL INVESTIGATION INTERVENTIONAL ONCOLOGY

Radiation Exposure of Abdominal Cone Beam Computed Tomography

Anna M. Sailer · Geert Willem H. Schurink · Joachim E. Wildberger · Rick de Graaf · Willem H. van Zwam · Michiel W. de Haan · Gerrit J. Kemerink · Cécile R. L. P. N. Jeukens

Received: 22 January 2014 / Accepted: 31 March 2014 / Published online: 6 May 2014

Abstract
Purpose To evaluate patients radiation exposure of abdominal C-arm cone beam computed tomography (CBCT).
Methods This prospective study was approved by the institutional review board; written, informed consent was waived. Radiation exposure of abdominal CBCT was evaluated in 40 patients who underwent CBCT during endovascular interventions. Dose area product (DAP) of CBCT was documented and effective dose (ED) was estimated based on organ doses using dedicated Monte Carlo simulation software with consideration of X-ray field location and patients' individual body weight and height. Weight-dependent ED per DAP conversion factors were calculated. CBCT radiation dose was compared to radiation dose of procedural fluoroscopy. CBCT dose-related risk for cancer was assessed.
Results Mean ED of abdominal CBCT was 4.3 mSv (95 % confidence interval [CI] 3.9; 4.8 mSv, range 1.1–7.4 mSv). ED was significantly higher in the upper than in the lower abdomen ($p = 0.003$) and increased with patients' weight ($r = 0.55$, slope = 0.045 mSv/kg, $p < 0.001$). Radiation exposure of CBCT corresponded to the radiation exposure of on average 7.2 fluoroscopy minutes (95 % CI 5.5; 8.8 min) in the same region of interest. Lifetime risk of exposure related cancer death was 0.033 % or less depending on age and weight.
Conclusions Mean ED of abdominal CBCT was 4.3 mSv depending on X-ray field location and body weight.

Keywords Cone beam computed tomography · Radiation dosage · Fluoroscopy · Radiation-induced cancer

A. M. Sailer (✉) · J. E. Wildberger · R. de Graaf · W. H. van Zwam · M. W. de Haan · G. J. Kemerink · C. R. L. P. N. Jeukens
Department of Radiology, Maastricht University Medical Centre (MUMC), P. Debyelaan 25, 6229 HX Maastricht, The Netherlands
e-mail: anni.sailer@mumc.nl

J. E. Wildberger
e-mail: j.wildberger@mumc.nl

R. de Graaf
e-mail: r.de.graaf@mumc.nl

W. H. van Zwam
e-mail: w.van.zwam@mumc.nl

M. W. de Haan
e-mail: m.de.haan@mumc.nl

G. J. Kemerink
e-mail: gerrit.kemerink@mumc.nl

C. R. L. P. N. Jeukens
e-mail: cecile.jeukens@mumc.nl

G. W. H. Schurink
Department of Surgery, Maastricht University Medical Centre, Maastricht, The Netherlands
e-mail: gwh.schurink@mumc.nl

Introduction

C-arm cone beam computed tomography (CBCT) is an advanced imaging technology that acquires volumetric "CT-like" images by flat panel detectors in state-of-the-art interventional angiography suites. Multiple viewing planes in three-dimensional (3D) datasets and enhanced soft-tissue contrast provide substantial improvement to conventional fluoroscopy and angiography [1]. In recent years, various clinical applications of CBCT have been evaluated for vascular and nonvascular interventional procedures and

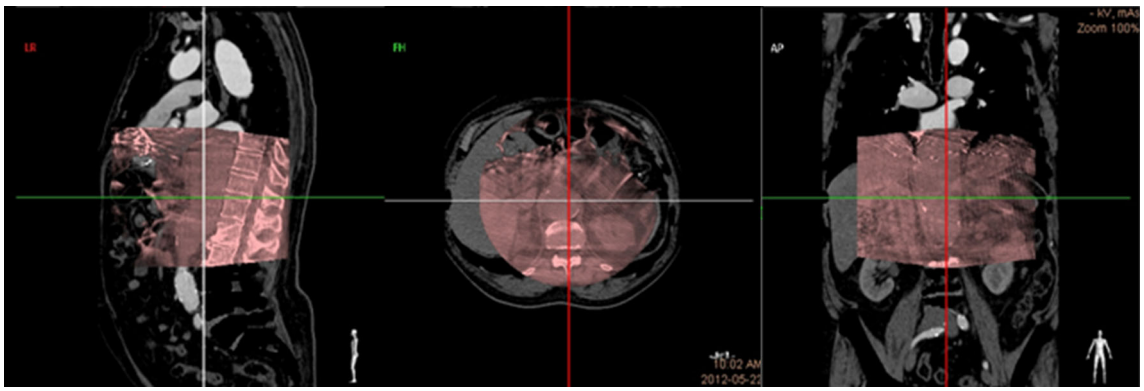

Fig. 1 Volumetric CBCT dataset (*pink*) coregistered to MDCT dataset (*grey*) in a patient with thoracoabdominal aortic aneurysm. CBCT was acquired in the patient's upper abdomen just before the intervention for image fusion guidance during BEVAR

reports of use emerge in medical literature. These include biopsy and ablation needle guidance [2–4], endovascular road-mapping and catheter guidance [5–9], immediate multiplanar posttreatment assessment [6, 10], and soft-tissue imaging [11, 12]. These features may enhance procedural efficacy and safety, but the body of data on radiation exposure is still limited.

CBCT should not result in additional radiation exposure for the medical staff, as all members are usually outside the interventional suite during acquisition. For patients, the application of CBCT may lead to an increase of procedural exposure to radiation, but a net reduction of fluoroscopy time and angiogram series due the availability of better spatial information also is possible [5, 13]. (Nonuniform) exposure to ionizing radiation can be assessed in terms of equivalent organ doses and effective dose (ED), which are expressed in units of Sievert, typically in the millisievert (mSv) range. The organ doses allow an estimation of the attributable risk to develop lethal malignancy later in life [14, 15]. The purpose of our study was to evaluate patients' radiation exposure of abdominal C-arm CBCT.

Materials and Methods

This prospective study was approved by the institutional review board; informed consent was waived. CBCT radiation exposure was prospectively evaluated in patients with thoracoabdominal aneurysms and other complex vascular diseases who underwent fenestrated or branched endovascular aortic repair (FEVAR/BEVAR) or endovascular recanalization and stenting procedures between June 2012 and August 2013. In all patients, CBCT was performed before the intervention for image fusion guidance. Figure 1 shows an example of abdominal CBCT coregistered to multidetector computed tomography (MDCT) angiography.

Acquisitions

Abdominal CBCT was acquired at our angiography suite through rotational movement of the C-arm covering a 180° circular under couch trajectory (Allura Xper FD20, Philips Healthcare, Best, The Netherlands). Volumetric datasets were automatically sent to a 3D workstation for multiplanar viewing and image coregistration. All technical parameters of the CBCT acquisition are summarized in Table 1. Standard parameters of fluoroscopic imaging were a total beam filtration of 0.4-mm copper and 3.5-mm aluminum, 15 frames per second, and automatic exposure control (AEC).

Radiation Exposure Analysis

For all procedures, radiation exposure of the CBCT run and total procedure in terms of dose area product (DAP; in $Gycm^2$) as well as total procedural fluoroscopy time were registered in the fluoroscopy unit's radiation dose report. For the last 17 procedures, standardized radiation dose structured reporting (RDSR) had become available wherein the DAP values of procedural fluoroscopy were also registered. Patients' individual body weight and height at the date of the intervention were documented. Precise CBCT X-ray field location was displayed on the scout image of each CBCT run. CBCT X-ray field was focused on the upper abdomen in 24 patients and on the lower abdomen in 16. Figure 2 demonstrates exemplary the X-ray field and included organs for upper and lower abdominal CBCT as drawn on the PCXMC phantom.

Effective Dose Estimation

The ED was estimated by means of a dedicated Monte Carlo software program (PCXMC v2.0, STUK, Helsinki, Finland) in which a size adjustable mathematical

Table 1 Technical parameters of abdominal CBCT acquisition with automatic exposure control

Parameter	Abdominal CBCT
Name	CT abdomen LD roll
Tube voltage	117–123 kV*
Tube current	142–325 mA*
mAs value	269–1027 mAs*
Pulse width	6–10 ms*
Speed	30 frames/s
Exposure/acquisition time	10.5 s
Angle of image acquisition	180°
Number of projections	316
Source–image distance	120 cm
Focus–isocenter distance	81 cm
Inherent filtration	2.5-mm aluminum equivalent
Added filtration	1-mm aluminum + 0.9-mm copper
Detector	Dynamic Flat Panel, Trixell, Pixium 4700
Image matrix	2480 × 1910 pixels
Pixel pitch	154 µm
Detector size	30 × 38 cm
Field of view CBCT (height × width × depth)	19 × 25 × 25 cm
Reconstructed slice thickness	0.98 mm

* Values depend on body characteristics and vary during acquisition due to automatic exposure control

hermaphrodite phantom model is used (Fig. 2). The phantom incorporates 29 different organs and tissues for which organ doses can be calculated under consideration of patient size, exposure geometry, and beam quality. With PCXMC software, organ doses were calculated for every patient separately based on CBCT technical parameters (Table 1) and patients' individual DAP values and body characteristics. To this extent, the 180° rotation was divided into 19 projections with a 10° increment each. For each angle, we ensured that the center of the (hermaphrodite) software phantom remained in the isocenter of rotation, i.e., the focus-skin distance and entrance field size were adjusted according to the thickness of the phantom. The equivalent dose of all organs was estimated by the software for each projection using 1/19 of the total CBCT DAP value. The corresponding ED was calculated by means of ICRP 103 tissue weighting factors [14]. Total ED of CBCT represents the sum of the 19 projections. Calculations were separately repeated for each patient with adjustment of patient's individual body weight and height as well as precise CBCT X-ray field location and mean individual kV value. Weight-dependent ED per DAP conversion factors and their variation with projection angles were calculated.

Comparison of CBCT with Fluoroscopy

The average fluoroscopy time corresponding to a radiation exposure equivalent to the radiation exposure of the CBCT was estimated for each patient individually by dividing the CBCT DAP by the fluoroscopy DAP rate. The fluoroscopy DAP rate is calculated as the total fluoroscopy DAP divided by the total fluoroscopy time.

Assessment of Exposure Related Cancer Risk

Assessment of the cancer risk due to CBCT exposure was performed using the PCXMC software. The risk estimates are based on the organ doses, organ-specific risk factors, patient age, and risk models established by the Biological Effects of Ionizing Radiation (BEIR) VII committee [15] resulting in the risk of exposure induced death (REID).

Statistical Analysis

Differences in radiation exposure and patient characteristics between upper and lower abdominal CBCT were tested on statistical significance using the independent samples *t* test (SPSS statistics 20.0, Chicago, IL). Correlations between patients' body weight and height and CBCT radiation exposure and equivalent fluoroscopy time were examined using linear regression. Two-sided *p* values <0.05 were considered significant.

Results

The study group consisted of 27 male and 13 female patients with a mean ± SD age of 68 ± 12 years and mean ± SD body mass index (BMI) of 26.7 ± 5.1 kg/m^2. Table 2 gives an overview of the average organ doses for the CBCT run and standard error of the mean as well as associated tissue weighting factors [14]. The radiation dose was highest in the kidneys, spleen, adrenals, pancreas, and liver for upper abdominal CBCT and by ovaries, uterus, colon, small intestine, urinary bladder, and active bone marrow for lower abdominal CBCT. Table 3 provides summarized results of CBCT radiation exposure estimation. ED of the CBCT run was estimated to be in the range of 1.1–7.4 mSv. Mean ED for upper abdominal CBCT was 4.9 mSv (95 % confidence interval [CI] 4.3–5.4 mSv) and mean ED for lower abdominal CBCT was 3.5 mSv (95 % CI 3.0–4.1 mSv); differences between upper and lower abdominal X-ray field location were statistically significant ($p = 0.003$).

There was a significant positive correlation between DAP value and body weight (Fig. 3A; r = 0.76, slope

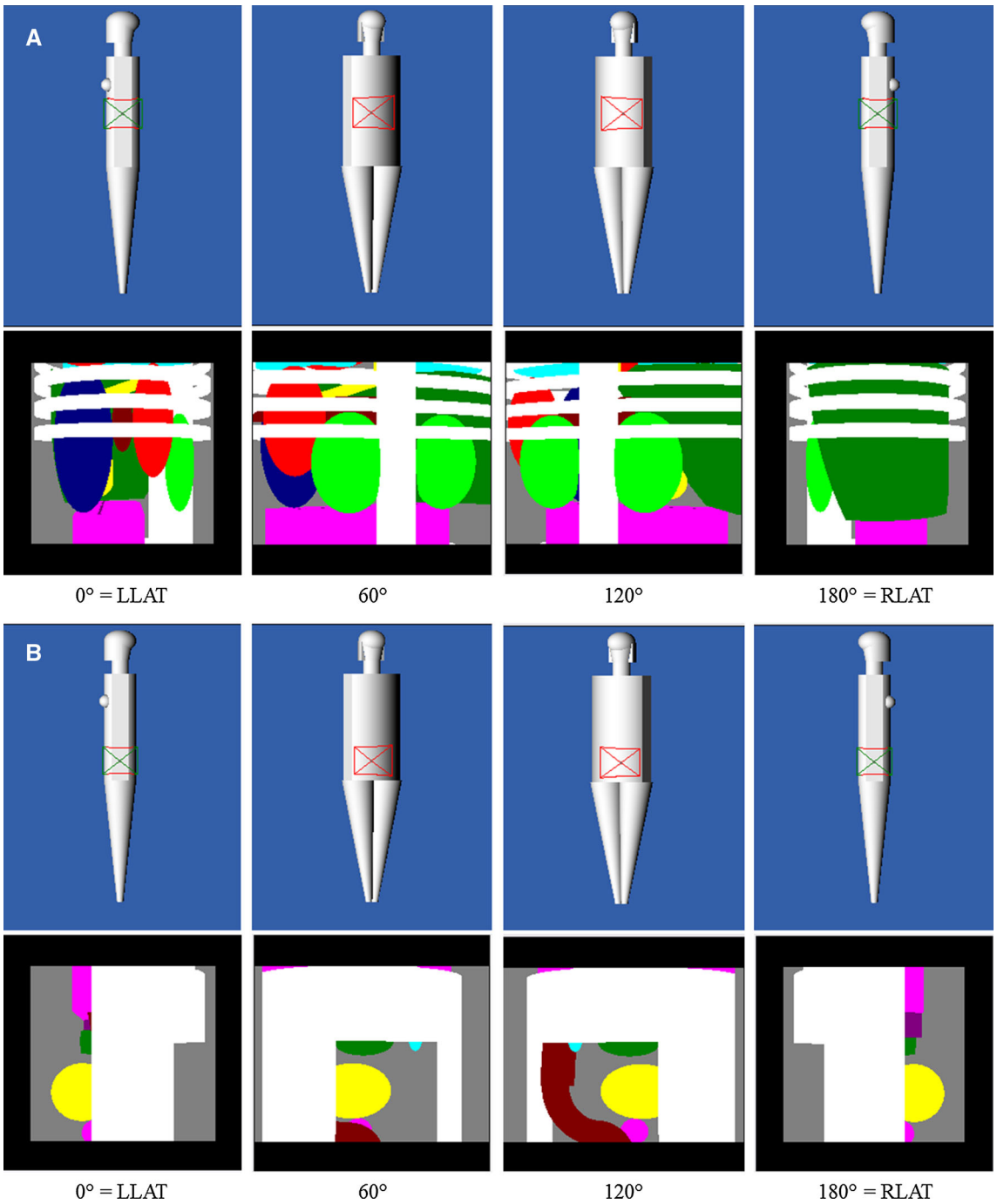

Fig. 2 *Upper rows* Projection of the X-ray field on the PCXMC phantom exemplary shown for 4 of the 19 steps. *Bottom rows* schematic representation of the organs present in each projection. Organs included in upper abdominal CBCT X-ray field **A** lung base (*light blue*), heart (*red*), stomach (*dark blue*), distal esophagus (*yellow*), liver (*dark green*), spleen (*red*), pancreas (*brown*), kidneys and adrenals (*light green*), colon (*pink*), small intestine (*pink*), gallbladder (*yellow*), and skeleton (*white*). Organs included in lower abdominal CBCT X-ray field **B** colon (*brown*), small intestine (*pink*), urinary bladder (*yellow*), female and male reproductive organs (*red*, *green*, and *light blue*), prostate (*pink*), and skeleton (*white*). *LLAT* left lateral detector position; *RLAT* right lateral detector position

0.238 $Gycm^2/kg$, $p < 0.001$) as well as ED and body weight (Fig. 3B; r = 0.55, slope = 0.045 mSv/kg, $p < 0.001$). The conversion factor ED per DAP decreased with increasing body weight (Fig. 3C; r = 0.99, slope = -0.00279 $mSv/Gycm^2kg$, $p < 0.001$ for upper abdominal CBCT and r = 0.99 slope = -0.00197 $mSv/Gycm^2kg$, $p < 0.001$ for lower abdominal CBCT). Adding patients' body height as an independent variable into the regression models yielded no significant regression coefficients for height ($p > 0.05$).

Table 2 Mean equivalent organ doses and standard error of the mean for upper and lower abdominal CBCT and associated tissue weighting factors (IRCP 103) exemplary for mean patient size (170 cm, 78 kg) and associated DAP value (14.7 Gycm^2)

Organ	Upper abdominal CBCT mean dose ± SE (mGy)	Lower abdominal CBCT mean dose ± SE (mGy)	TWF IRCP 103
Active bone marrow	5.07 ± 0.71	8.92 ± 0.8	0.12
Adrenals	24.22 ± 1.56	0.34 ± 0.12	0.009
Brain	0 ± 0	0 ± 0	0.01
Breasts	0.64 ± 0.11	0.03 ± 0.02	0.12
Colon	4.68 ± 1.44	10.4 ± 1.38	0.12
Esophagus	4.8 ± 0.59	0.12 ± 0.05	0.05
Extrathoracic airways	0.03 ± 0.01	0 ± 0	0.009
Gallbladder	11.43 ± 2.16	1.68 ± 0.28	0.01
Heart	2.79 ± 0.39	0.09 ± 0.04	0.011
Kidneys	32.79 ± 1.57	1.38 ± 0.29	0.012
Liver	15.14 ± 2.18	0.59 ± 0.13	0.05
Lung	2.8 ± 0.32	0.07 ± 0.03	0.12
Lymph nodes	6.05 ± 1.12	3.11 ± 0.36	0.009
Muscle	3.21 ± 0.51	4.52 ± 0.7	0.009
Oral mucosa	0.02 ± 0	0 ± 0	0.009
Ovaries	1.55 ± 0.55	17.28 ± 1.99	0.04
Pancreas	15.52 ± 2.14	0.64 ± 0.17	0.009
Prostate	0.18 ± 0.09	8.78 ± 2.04	0.005
Salivary glands	0.02 ± 0.01	0 ± 0	0.01
Skeleton	4.14 ± 0.49	5.15 ± 0.81	0.00
Skin	2.27 ± 0.32	2.65 ± 0.41	0.01
Small intestine	6.16 ± 2.12	10.26 ± 1.15	0.009
Spleen	24.94 ± 2.77	0.56 ± 0.16	0.009
Stomach	11.45 ± 1.99	0.87 ± 0.17	0.12
Testicles	0.04 ± 0.02	1.9 ± 1.02	0.04
Thymus	0.55 ± 0.1	0.02 ± 0.01	0.009
Thyroid	0.07 ± 0.02	0 ± 0	0.05
Urinary bladder	0.39 ± 0.15	9.65 ± 1.71	0.05
Uterus	1.29 ± 0.48	14.6 ± 1.9	0.005

TWF tissue weighting factor

Radiation exposure of CBCT corresponded to the radiation exposure of on average 7.2 minutes (95 % CI 5.5–8.8 min) live fluoroscopy in the same region of interest. CBCT dose equivalent fluoroscopy time increased significantly with weight (r = 0.53, slope = 0.188 min/kg, $p = 0.034$).

Calculated risk of CBCT exposure-induced death based on organ doses for various cancer types is shown in Fig. 4 as a function of age and body weight. For example, for a 60-year-old female patient with a body weight of 78 kg, the stochastic risk for exposure-related cancer death was 0.0182 % for upper abdominal CBCT and 0.0147 % for lower abdominal CBCT, respectively. Calculated maximum risk for lifetime exposure induced death was 0.033 %.

Discussion

We prospectively evaluated the patient's radiation exposure in 40 abdominal CBCT runs by means of dedicated Monte Carlo modelling. Organs positioned in the X-ray field received the highest dose. Average ED of CBCT was 4.3 (range 1.1–7.4) mSv. Patient's radiation exposure of abdominal CBCT equals approximately 1.8–2.7 times the annual background radiation dose worldwide and the Netherlands (2.4 and 1.6 mSv respectively, excluding doses for medical purposes) [15, 16] and approximately half of the ED of abdominal MDCT (8 mSv, values reported between 3.5 and 25 mSv) [17, 18]. There was a significant relationship towards lower ED in CBCT with the X-ray field in the lower abdomen compared with upper abdomen ($p = 0.003$) and a strong significant positive correlation between ED and body weight ($p < 0.001$). For correct interpretation of the ED values, one must realize the uncertainties present in such estimations. Because ED and organ doses cannot be measured in vivo, different approaches are followed. In MDCT, dose estimations are often performed by means of CT dose index (CTDI). Due to the smaller in-plane field of view and larger scan range of CBCT compared with MDCT, the CTDI values are not applicable for CBCT [19, 20]. A more accurate method, in line with the definition of ED, is to estimate the organ doses and subsequently calculate the ED using tissue weighting factors [14]. The organ doses can be measured using an anthropomorphic phantom with integrated thermoluminescent dosimeters (TLDs), or using the DAP value (displayed by the angiography system) and Monte Carlo software. Main disadvantage of a dosimeter phantom is that the conversion factor ED per DAP does not account for differences in body characteristics, whereas our data show that there is a strong weight dependency for the conversion factor. Furthermore, the phantom might not be representative for the actual patient population as illustrated in the TLD phantom study from Tyan et al. [20] evaluating CBCT in liver embolization in the Taiwan population. They observed much higher DAP values in their patients compared to the phantoms.

To achieve the best possible estimation of the ED of CBCT runs, we performed separate PCXMC Monte Carlo calculations for each patient while precisely accounting for individual CBCT X-ray field location and body characteristics. Moreover, we divided the 180° CBCT run into 19 projection angles, thereby compensating for the varying

Table 3 Results of CBCT radiation exposure estimation and impact on total procedure DAP as well as fluoroscopy time equivalence to CBCT

	All					Upper abdominal CBCT					Lower abdominal CBCT					*p* value
	Mean	95 % CI		Min	Max	Mean	95 % CI		Min	Max	Mean	95 % CI		Min	Max	Upper vs. lower abdomen
Patients																
Number of patients (male/female)	40 (27/13)					24 (20/4)					16 (7/9)					
Body weight (kg)	78	72	83	40	125	80	73	87	40	125	74	67	82	50	108	0.32
Body length (cm)	170	167	174	130	198	174	170	178	157	198	165	160	171	130	183	0.022
BMI (kg/m^2)	26.7	25.1	28.3	16.0	43.3	26.4	24.4	28.4	16.0	39.9	27.2	24.6	29.8	18.1	43.3	0.619
CBCT																
DAP (Gycm^2)	14.7	13.0	16.4	3.7	25.6	14.7	12.6	16.9	4.8	25.6	14.5	11.6	17.4	3.7	23.8	0.901
ED per DAP (mSv per Gycm^2)	0.31	0.29	0.33	0.19	0.48	0.34	0.32	0.37	0.24	0.48	0.25	0.24	0.27	0.19	0.31	<0.001
Effective dose (mSv)	4.3	3.9	4.8	1.1	7.4	4.9	4.3	5.4	2.3	7.4	3.5	3.0	4.1	1.1	6.0	0.003
Total Procedure																
Total DAP (Gycm^2)	217	159	276	15	699	286	210	361	48	699	114	46	182	15	501	0.003
Proportion CBCT on total procedure DAP	12.9 %	9.8 %	16.0 %	1.9 %	34.1 %	7.3 %	5.3 %	9.3 %	1.9 %	20.5 %	21.4 %	16.4 %	26.2 %	4.4 %	34.1 %	<0.001
Comparison CBCT – fluoroscopy																
Number of patients (male/female)	17 (9/8)					5 (4/1)					12 (5/7)					
Cumulative fluoroscopy time	22 min 55 s	10 min 8 s	35 min 2 s	4 min 1 s	93 minv41 s	56 min 5 s	35 min 2 s	77 min 9 s	30 min 28 s	93 min 41 s	9 min 5 s	6 min 10 s	12 min 0 s	4 min 1 s	19 min 44 s	0.011
DAP fluoroscopy (Gycm^2)	42.8	20.9	64.7	3.1	147.4	104.1	70.5	137.6	73.2	147.4	17.3	10.7	23.8	3.1	37.4	0.006
DAP rate (mGycm^2/s)	32.3	25.9	38.7	9.8	61.3	32.5	24.5	40.5	22.6	43.6	32.2	23.6	40.8	9.8	61.3	0.968
Fluoroscopy time equivalent to CBCT dose	7 min 12 s	5 min 30 s	8 min 48 s	3 min 12 s	15 min 12 s	7 min 42 s	4 min 30 s	10 min 54 s	3 min 12 s	12 min 24 s	7 min 0 s	5 min 0 s	8 min 54 s	3 min 12 s	15 min 12 s	0.708

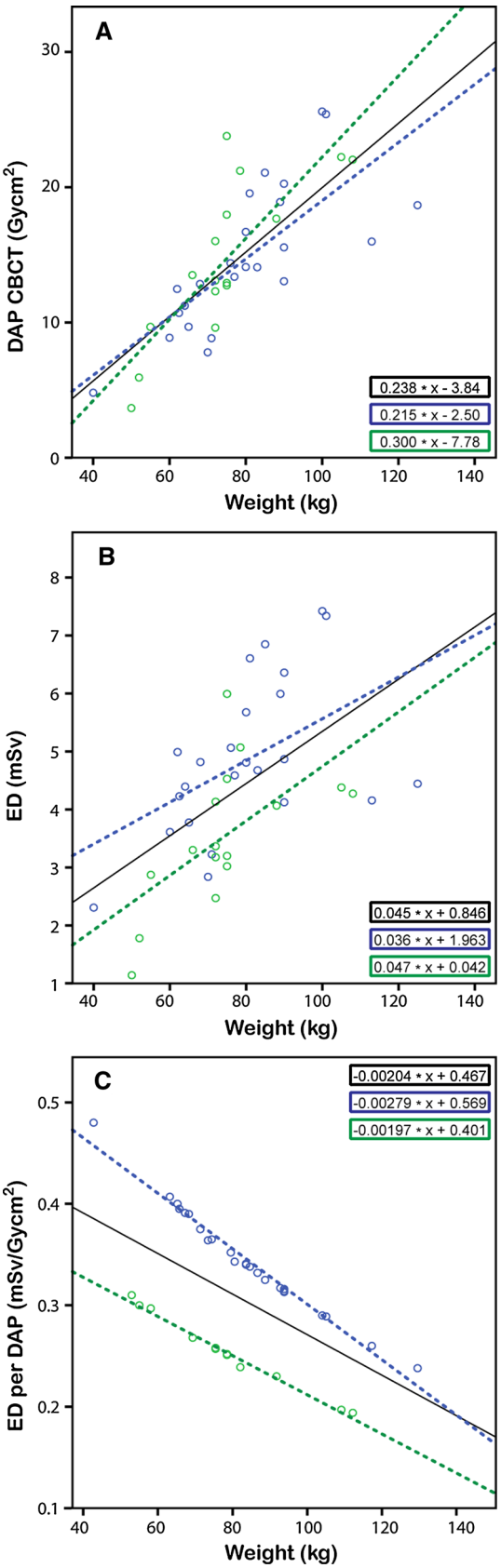

◀**Fig. 3** Correlation between **A** DAP value versus body weight **B** ED versus body weight and **C** ED per DAP versus body weight for upper and lower abdominal CBCT. *Blue symbols* and *lines* upper abdominal CBCT. *Green symbols* and *lines* lower abdominal CBCT. *Black lines* all CBCT

phantom thickness by adjusting the focus-skin distance and entrance field size. A limitation is that this method does not incorporate the dose and kV-modulation during the CBCT rotation by the AEC as a result of varying body geometry (i.e., the body is thicker in lateral projection compared to PA/AP). To estimate the error introduced, we assessed the angular dependence of DAP and high-voltage during CBCT acquisition by performing separate experiments on an Alderson Rando abdominal phantom, whereas DAP-rate and kV were dynamically recorded on video tape as displayed during rotation. ED was recalculated using the obtained nonuniform DAP and kV distribution showing that uniformly distributed DAP values and the fixed high-voltage overestimate the ED by 3.0 %.

Prior research has been performed on CBCT radiation exposure. Suzuki et al. performed a TLD phantom study and Monte Carlo simulations based on phantom DAP values to assess the radiation exposure of upper abdominal CBCT in three different angiography units (Siemens Artis dTA, Philips Allura Xper, GE Innova 4100). In the Monte Carlo simulations, they evaluated 13 projection angles and calculated ED per DAP conversion factors using the former ICRP 60 tissue weighting factors. Doses were estimated for three different phantom sizes. ED of upper abdominal CBCT in a medium size phantom (BMI 23.1 kg/m^2) was reported to be in the range from 2.4 to 3.1 mSv, depending on the angiography unit's CBCT technical parameters. Largest dose difference between CBCT protocols from different angiography units was 0.8 mSv [21]. Analogously to our results, they found a decreasing conversion factor ED per DAP for increasing phantom size. Other studies reported the ED of abdominal CBCT to be in the range from 3.5 to 25.4 mSv; however, these results are based on phantom studies or lack detailed information on dose estimation method [6, 12, 22–25].

Exposure to ionizing radiation introduces risk of developing cancer. The ICRP has established the lifetime detriment adjusted risk coefficient for cancer in the whole population, i.e., comprised of all ages, to be 5.5 % per unit Sievert [14]. Such a risk estimation based on the ED exhibits inaccuracies as is does not account for age at exposure, current age, or body region exposed. We therefore performed accurate risk estimations using the PCXMC software that incorporates organ doses, age, and organ-specific risk factors [15], expressed in lifetime risk of exposure induced cancer death. The risk of overall cancer incidence is approximately a factor two higher, although

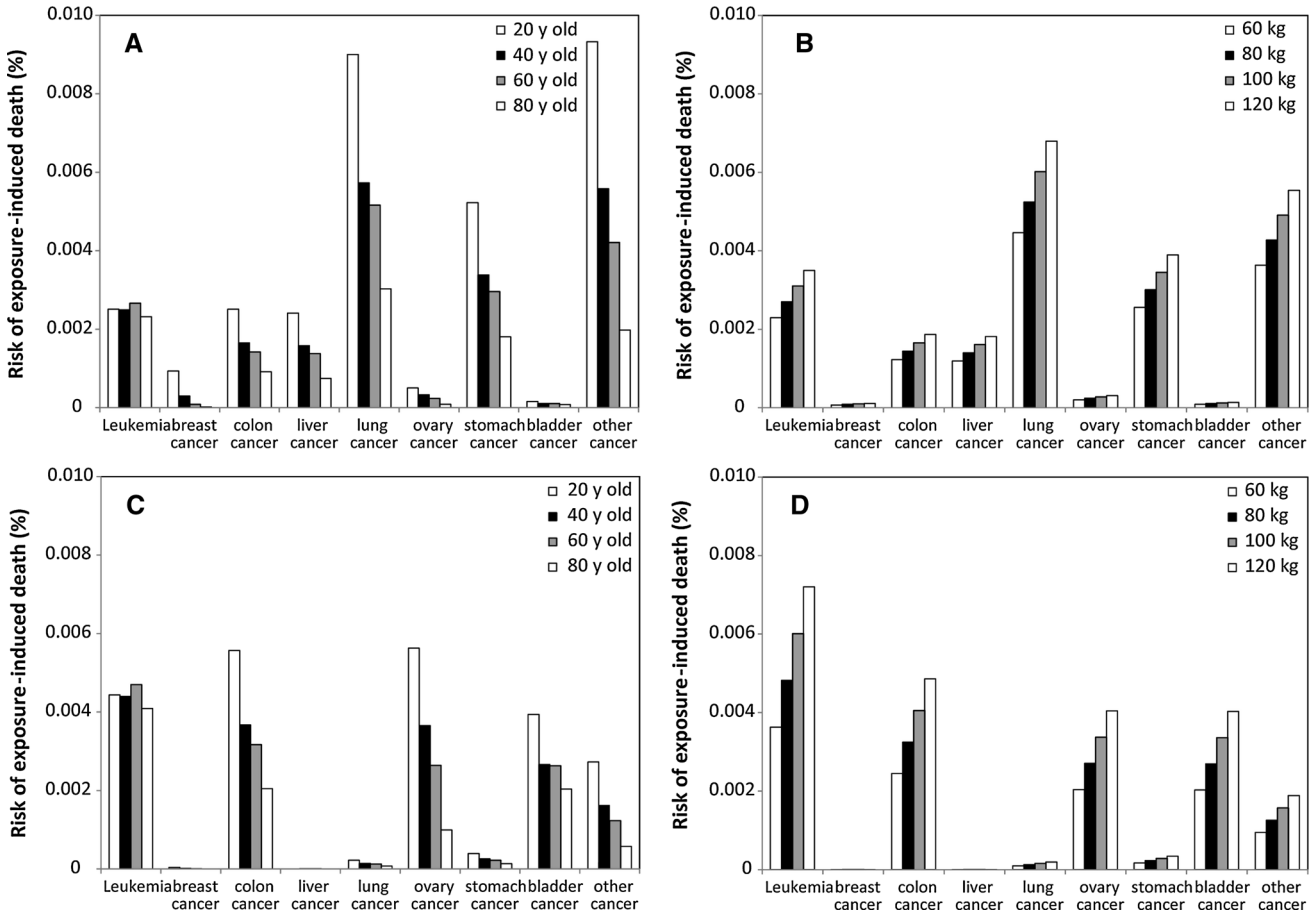

Fig. 4 Risk for exposure-induced lethal cancer types for upper abdominal CBCT (**A**, **B**) and lower abdominal CBCT (**C**, **D**) based on individual organ doses as a function of age (**A**, **C**, weight = 80 kg) and weight (**B**, **D**, age = 60 years)

this varies for specific cancer types according to their lethality [15]. The stochastic model for cancer risks below 100 mSv has to be interpreted with caution. The BEIR VII committee reports 95 % confidence intervals for overall cancer mortality and incidence showing that the risks can be estimated within a factor of two [15]. This means that it is prudent to interpret the lifetime attributable risk (LAR) as an order of magnitude rather than an absolute number. Risk of cancer due to the CBCT radiation exposure is very low compared with natural cancer incidence, which is 37–46 %, and natural risk of lethal cancer, which is 18–22 % or one out of five for the U.S. population [15]. To put CBCT radiation in perspective, we performed PXCMC analysis for the whole procedures. In our patient population, mean radiation exposure for FEVAR/BEVAR procedures was 84.9 mSv (95 % CI 62.3–107.2 mSv) and 26.5 mSv (95 % CI 10.7-42.2 mSv) for pelvic procedures. Corresponding risk of cancer therefore was factor 17 and 8 higher respectively compared to the risk from only CBCT exposure. Furthermore, CBCT radiation has to been seen in the context of the vascular disease management as this patient population is expected to undergo further MDCT during follow-up or may undergo reinterventions, which summarizes considerable lifetime dose.

As any new exposure, CBCT-related radiation has to be discussed in the context of the basic safety principle, i.e., to keep any radiation exposure As Low As Reasonably Achievable (ALARA). CBCT technology might contribute to enhance procedural efficacy and reduce procedural fluoroscopy time. The medical staff is normally in a protected area during CBCT. Therefore, any reduction in fluoroscopy due to the application of CBCT might lead to a welcome reduction of dose incurred by interventional radiologists.

In conclusion, ED of abdominal CBCT corresponds to approximately half of the dose of abdominal MDCT. Application of CBCT will result in a reduction of patients total procedural radiation exposure if a reduction of fluoroscopy time of approximately 7 min is achieved.

Conflict of interest Anna M. Sailer, Geert Willem H. Schurink, Joachim E. Wildberger, Rick de Graaf, Willem H. van Zwam, Michiel W. de Haan, Gerrit J. Kemerink and Cécile R. L. P. N. Jeukens have no conflict of interest.

References

1. Wallace MJ, Kuo MD, Glaiberman C, Binkert CA, Orth RC, Soulez G (2008) Three-dimensional C-arm cone-beam CT: applications in the interventional suite. J Vasc Interv Radiol 19(6):799–813
2. Krücker J, Xu S, Venkatesan A, Locklin JK, Amalou H, Glossop N, Wood BJ (2011) Clinical utility of real-time fusion guidance for biopsy and ablation. J Vasc Interv Radiol 22(4):515–524
3. Braak SJ, van Strijen MJ, van Leersum M, van Es HW, van Heesewijk JP (2010) Real-time 3D fluoroscopy guidance during needle interventions: technique, accuracy, and feasibility. AJR Am J Roentgenol 194(5):W445–W451
4. Meyer BC, Brost A, Kraitchman DL, Gilson WD, Strobel N, Hornegger J, Lewin JS, Wacker FK (2013) Percutaneous punctures with MR imaging guidance: comparison between MR imaging-enhanced fluoroscopic guidance and real-time MR Imaging guidance. Radiology 266(3):912–919
5. Sailer AM, de Haan MW, Peppelenbosch AG, Jacobs MJ, Wildberger JE, Schurink GW (2014) CTA with fluoroscopy image fusion guidance in endovascular complex aortic aneurysm repair. Eur J Vasc Endovasc Surg. doi:10.1016/j.ejvs.2013.12.022.Epub
6. Dijkstra ML, Eagleton MJ, Greenberg RK, Mastracci T, Hernandez A (2011) Intraoperative C-arm cone-beam computed tomography in fenestrated/branched aortic endografting. J Vasc Surg 53(3):583–590
7. Kobeiter H, Nahum J, Becquemin JP (2011) Zero-contrast thoracic endovascular aortic repair using image fusion. Circulation 124(11):e280–e282
8. Deschamps F, Solomon SB, Thornton RH, Rao P, Hakime A, Kuoch V, de Baere T (2010) Computed analysis of three-dimensional cone-beam computed tomography angiography for determination of tumor-feeding vessels during chemoembolization of liver tumor: a pilot study. Cardiovasc Interv Radiol. doi:10.1007/s00270-010-9846-6
9. Tam A, Mohamed A, Pfister M, Rohm E, Wallace MJ (2009) C-arm cone beam computed tomographic needle path overlay for fluoroscopic-guided placement of translumbar central venous catheters. Cardiovasc Interv Radiol 32(4):820–824
10. Benndorf G, Strother CM, Claus B, Naeini R, Morsi H, Klucznik R, Mawad ME (2005) Angiographic CT in cerebrovascular stenting. AJNR Am J Neuroradiol 26(7):1813–1818
11. Möhlenbruch M, Nelles M, Thomas D, Willinek W, Gerstner A, Schild HH, Wilhelm K (2010) Cone-beam computed tomography-guided percutaneous radiologic gastrostomy. Cardiovasc Interv Radiol 33(2):315–320
12. Aadland TD, Thielen KR, Kaufmann TJ, Morris JM, Lanzino G, Kallmes DF, Schueler BA, Cloft H (2010) 3D C-arm cone-beam CT angiography as an adjunct in the precise anatomic characterization of spinal dural arteriovenous fistulas. AJNR Am J Neuroradiol 31(3):476–480
13. Schafer S, Nithiananthan S, Mirota DJ, Uneri A, Stayman JW, Zbijewski W, Schmidgunst C, Kleinszig G, Khanna AJ, Siewerdsena JH (2011) Mobile C-arm cone-beam CT for guidance of spine surgery: image quality, radiation dose, and integration with interventional guidance. Med Phys 38(8):4563–4574
14. Valentin J (2007) The 2007 recommendations of the International Commission on Radiological Protection, Annals of the ICRP publication 103. Elsevier Science, Oxford
15. Committee to Assess Health Risks from Exposure to Low Levels of Ionizing Radiation NRC (2006) Health risks from exposure to low levels of ionizing radiation: BEIR VII phase 2. National Academic Press, Washington DC
16. Rijksinstituut voor Volksgezondheid en Milieu, Ministerie van Volksgezondheid, Welzijn en Sport (2013) Stralingsbelasting in Nederland/Aandeel per stralingsbron. http://www.rivm.nl/Onderwerpen/S/Stralingsbelasting_in_Nederland/Aandeel_per_stralingsbron. Accessed 09 Jan 2014
17. Mettler FA Jr, Huda W, Yoshizumi TT, Mahesh M (2008) Effective doses in radiology and diagnostic nuclear medicine: a catalog. Radiology 248(1):254–263
18. van der Molen AJ, Schilham A, Stoop P, Prokop M, Geleijns J (2013) A national survey on radiation dose in CT in The Netherlands. Insights Imaging 4(3):383–390
19. Li J, Udayasankar UK, Toth TL, Seamans J, Small WC, Kalra MK (2007) Automatic patient centering for MDCT: effect on radiation dose. AJR Am J Roentgenol 188(2):547–552
20. Tyan YS, Li YY, Ku MC, Huang HH, Chen TR (2013) The effective dose assessment of C-arm CT in hepatic arterial embolisation therapy. Br J Radiol 86(1024):20120551
21. Suzuki S, Yamaguchi I, Kidouchi T, Yamamoto A, Masumoto T, Ozaki Y (2011) Evaluation of effective dose during abdominal three-dimensional imaging for three flat-panel-detector angiography systems. Cardiovasc Interv Radiol 34(2):376–382
22. Bai M, Liu B, Mu H, Liu X, Jiang Y (2012) The comparison of radiation dose between C-arm flat-detector CT (DynaCT) and multi-slice CT (MSCT): a phantom study. Eur J Radiol 81(11):3577–3580
23. Kwok YM, Irani FG, Tay KH, Yang CC, Padre CG (2013) Tan BS (2013) Effective dose estimates for cone beam computed tomography in interventional radiology. Eur Radiol 23(11):3197–3204. doi:10.1007/s00330-013-2934-7.Epub
24. Braak SJ, van Strijen MJL, van Es HW, Nievelstein RAJ, van Heesewijk JPM (2011) Effective dose during needle interventions: Cone-Beam CT guidance compared with conventional CT guidance. J Vasc Interv Radiol 22:455–461
25. Eide KR, Ødegård A, Myhre HO, Lydersen S, Hatlinghus S, Haraldseth O (2009) DynaCT during EVAR–a comparison with multidetector CT. Eur J Vasc Endovasc Surg 37(1):23–30